Fabrication of Magnetic Core–Shell $CoFe_2O_4/Al_2O_3$ Nanoparticles as Immobilized Metal Chelate Affinity Support for Protein Adsorption

Dian Quan Tang,[1] Da Jun Zhang,*[1] Dian Yong Tang,[2] and Hua Ai[3]
[1]*Research Institute of Education Science, Southwest University, Chongqing 400700, P. R. China*
[2]*College of Chemistry and Chemical Engineering, Sichuan University, Chengdu 610000, P. R. China*
[3]*Research Institute of Immunology and Psychology, Chengdu 610000, P. R. China*

(Received June 26, 2006; CL-060716; E-mail: tangdq@swu.edu.cn)

This study introduced the fabrication of core–shell magnetic $CoFe_2O_4/Al_2O_3$ nanocomposites as the immobilized affinity support for the detection of interleukin-6, as a model protein, in clinical immunoassay.

Many efforts have been made worldwide to develop and improve clinical immunoassays with the aim of making portable and affordable devices.[1] In spite of many advances in this field, it is still a challenge to find new approaches that could improve the simplicity, selectivity, and sensitivity of clinical immunoassay, in order to respond to the demands and needs of modern medical diagnostics and biomedical research applications.[2] In this regard, protein-mediated assembly of nanoparticles is a potent tool for preparation of new materials, which combine tunable nanoparticle features (size, surface functionality, and core properties) with the unique physical and chemical properties of protein and peptides.[3] This approach, however, has been limited to the synthetic modification of the nanoparticle to directly interact with antibody or protein-recognition sites.[4] An alternative strategy would be to target the surface of the protein through complementary interactions, using the shape and physical characteristics of the protein to dictate the structural feature in the resulting nanoparticle and protein composites.[5]

Herein, we synthesized a novel core–shell magnetic nanostructure material (i.e. $CoFe_2O_4/Al_2O_3$) for controlled protein–nanoparticle composite based on protein stability. $CoFe_2O_4$ is a well-known hard magnetic material with a very high magnetocrystalline anisotropy, high coercivity, and moderate saturation magnetization, which make it a promising material for high-density magnetic recording.[6] The fabrication of spinel ferrite nanoparticles has been investigated intensively in recent years because of their remarkable electrical and magnetic properties and wide practical applications for the development of biosensors, biofuel cell, biomaterial-based computers, and bioelectronic devices via magnetic control with an external magnet.[7] Al_2O_3 nanoparticles are a hydrophilic, porous, positively charged sol–gel matrix, which not only possesses the general advantages of sol–gel but also is an effective promoter of the biosensor.[8] The porous inorganic sol–gel matrix possesses physical rigidity, chemical inertness, high photochemical, biodegradational and thermal stability and experiences negligible swelling in both aqueous and organic solutions, resulting in high protein loading and retaining the bioactivity of the immobilized protein to a large extent.[8]

At the first step, the $CoFe_2O_4$ nanoparticles were prepared according to the literature.[9] Briefly, $Fe(NO_3)_3 \cdot 9H_2O$, $Co(NO_3)_3 \cdot 6H_2O$, and Glycine (Gly) were dissolved in distilled water (Note: $Fe^{3+}/Co^{2+} = 2/1$, Gly/nitrate $= 4/1$, in molar ratio). After filtration, the attained red precursor solution has been heated until combustion reaction was appeared. The black loose powders (i.e. $CoFe_2O_4$ nanoparticles) were obtained after combustion for several seconds. The XRD measurement shows large peaks and broad higher diffraction patterns at 30.9, 35.4, 43.1, 56.9, and 62.4° at 2θ, which are typical peaks of a Co–ferrite oxide.[10] Because of the similar spinel structures of $CoFe_2O_4$ and γ-Fe_2O_3, however, XRD phase analysis might not effectively differentiate the two phases when peak broadening occurs for the nanocrystalline particles. To further confirm the phase purity of $CoFe_2O_4$ formed, these samples were characterized by Raman spectroscopy. From our experimental results, very weak peaks were observed in the range from 800 to 2000 cm^{-1} while three strong peaks were achieved at 416, 471, and 610 cm^{-1}, which are indicative of $CoFe_2O_4$.[11]

At the second step, the $CoFe_2O_4/Al_2O_3$ nanoparticles was fabricated.[8] 0.5 g of $CoFe_2O_4$ was put in the mixed solution containing 10 mL of ethanol, 50 mL of deionized water, a certain amount of surfactant, and 2 g of aluminum iospropoxide (Al(*i*-PrO_3)). After the mixture was stirred for 45 min at 80 °C, 1.2 mL of 1 M HCl was added. The mixture was heated to 90 °C to allow evaporation of the 2-propanol produced via hydrolysis. After refluxed for 16 h under 90 °C, the mixture was filtered, rinsed with deionized water and ethanol, dried at 150 °C for 2 h, and calcinated at 800 °C for 4 h to prepare the $CoFe_2O_4/Al_2O_3$ nanoparticles composite. The mean sizes were 45 and 55 nm for $CoFe_2O_4$ nanoparticles and the $CoFe_2O_4/Al_2O_3$ composite nanoparticles by TEM, respectively (Figure 1).

To investigate the performance of the magnetic core–shell $CoFe_2O_4/Al_2O_3$ nanoparticles, the composite nanoparticles were employed as immobilized affinity supports for interleukin-6 (IL-6) antibody absorption, as a model protein. Prior to experiment, we used quartz crystal microbalance (QCM) technique to evaluate the immobilized amount of IL-6 antibody on the quartz crystal surface according to the Sauerbrey equation[12]

$$\Delta F_x = -2.3 \times 10^{-6} F^2 \Delta M / A, \quad (1)$$

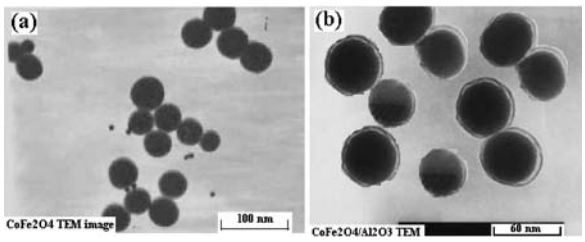

Figure 1. TEM micrographs of (a) $CoFe_2O_4$ nanoparticles and (b) magnetic $CoFe_2O_4/Al_2O_3$ core–shell nanoparticles.

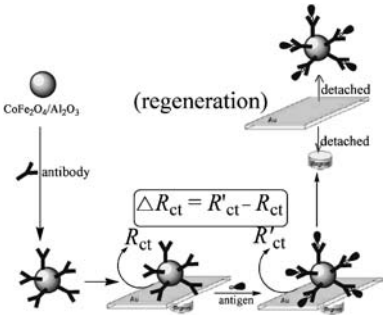

Figure 2. Schematic representation of the analytical protocol including the immobilization, measurement, and regeneration procedure of the immunosensor.

where ΔF_x is the resonant frequency difference (Hz); F is the basic resonant frequency of the crystal (MHz); ΔM is the mass accumulation on the crystal surface (g). A is the deposited electrode area (cm^2). The absorbed amount of IL-6 antibody was obtained through the mass change before and after the IL-6 antibody absorption on the composite nanoparticle surface. According to the Sauerbrey equation, the coverage of IL-6 antibody molecules on the quartz crystal surface was 5.9×10^{-8} mol·cm^{-2}.

Following that, a direct electrochemical immunoassay system was developed (Figure 2). To fabricate such an assay system, IL-6 antibodies were initially absorbed on the surface of magnetic nanocomposites, the antibody-modified magnetic nanocomposites were then attached onto the probe surface with the aid of a permanent magnet, Attraction of the functionalized magnetic nanoparticles to the probe surface activated the electrical contact between the immobilized antibodies and the base electrode, and the sensor's circuit is switched on. Positioning the magnet above the detection cell retracts the magnetic nanoparticles from the substrate surface, and the detection circuit is switched off, namely, achieved the regeneration of the immunosensors.

In order to investigate the possibility of the newly developed immunoassay system to be applied for clinical analysis, different concentrations of IL-6 standard samples were examined using the proposed immunosenosr via EIS technique. The measurement method is as follows: 30 μL of serum sample was added into the 70 μL of incubation solution (pH 7.0, PBS), and then the as-prepared immunosensor was incubated in the incubation solution at 35 °C for 60 min. After a washing step with doubly distilled water, the impedance measurement was carried out at the frequency range from 10^{-2} to 10^6 Hz at the formal potential of 220 mV with an alternating voltage of 10 mV. The principle of detection is based on the shift in electron-transfer resistance (R_{ct}) before and after the antigen–antibody reaction, i.e., $\Delta R_{ct} = R'_{ct} - R_{ct}$. As shown in Figure 3, a progressive increase in the impedance responses would be obtained with increasing the

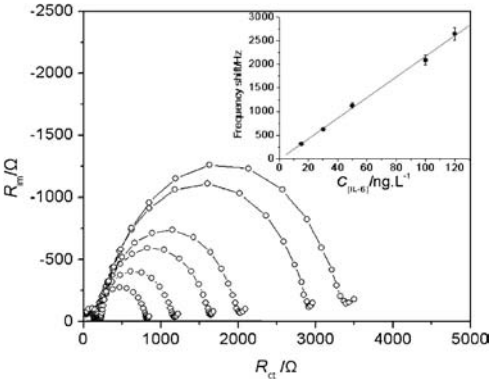

Figure 3. Electrochemical impedance spectroscopy (EIS) of the as-prepared immunosensor in 5 mM $Fe(CN)_6^{4-/3-}$ PBS (pH 7.0) after incubation with various IL-6 concentrations from 0 to 120 ng/L (from inner to outer). Inset: Calibration curve between the IL-6 concentration and frequency shift.

IL-6 concentration in incubation solution. A significant increase in the resistance could be attributed to the formation of the antigen–antibody complex. The data indicates that the immunosensor is capable of distinguishing IL-6 concentration range from 15 to 120 ng/L. Thus, the synthesized core–shell magnetic $CoFe_2O_4/Al_2O_3$ composite nanoparticles could be employed as the immobilized affinity support for the immobilization of antigen/antibody.

Although the present assay system is focused on detection of the target antigen molecules, it can be easily extended to other biosening systems, such as enzyme and DNA. Further investigations are going on to develop a microarray structure for our functional magnetic nanocomposite-based protein assay and to test them ultimate sensitivity.

References

1 I. Willner, E. Katz, *Angew. Chem., Int. Ed.* **2003**, *42*, 4576.
2 M. Sarikaya, C. Tamerler, A. K.-Y. Jen, K. Schulten, F. Baneyx, *Nat. Mater.* **2003**, *2*, 577.
3 P. Ringler, G. E. Schulz, *Science* **2003**, *302*, 106.
4 S. Connolly, D. Fitzmaurice, *Adv. Mater.* **1999**, *11*, 1202.
5 W. Shenton, D. Pum, U. B. Sleytr, S. Mann, *Nature* **1997**, *389*, 585.
6 M. H. Khedr, A. A. Omar, S. A. Abdel-Moaty, *Colloids Surf., A* **2006**, *281*, 8.
7 I. Willner, E. Katz. *Angew. Chem., Int. Ed.* **2003**, *42*, 4576.
8 Z. Liu, B. Liu, J. Kong, J. Deng, *Anal. Chem.* **2000**, *72*, 4707.
9 Z. Xu, F. Cheng, B. Zhou, C. Liao, C. Yan, *Chin. Sci. Bull.* **2001**, *46*, 384.
10 International Centre for Diffraction Data (ICDD), Powder Diffraction Database, Pattern 22–1086, **1994**.
11 M. H. Sousa, F. A. Tourinho, J. C. Rubim, *J. Raman Spectrosc.* **2000**, *31*, 185.
12 G. Sauerbrey, *Z. Phys.* **1959**, *155*, 2333.

Published on the web (Advance View) September 30, 2006; doi:10.1246/cl.2006.1238